International Journal of Minerals, Metallurgy and Materials
Volume 24, Number 6, June 2017, Page 718
DOI: 10.1007/s12613-017-1455-9

A strategy to obtain a high-density and high-strength zirconia ceramic via ceramic injection molding by the modification of oleic acid

Jia-xin Wen[1)], *Tian-bin Zhu*[2)], *Zhi-peng Xie*[2)], *Wen-bin Cao*[1)], *and Wei Liu*[3)]

1) School of Materials Science and Engineering, University of Science and Technology Beijing, Beijing 100083, China
2) Sate Key Laboratory of New Ceramics and Fine Processing, Department of Materials Science and Engineering, Tsinghua University, Beijing 100084, China
3) School of Electromechanical Engineering, Guangdong University of Technology, Guangzhou 510006, China
(Received: 27 October 2016; revised: 26 December 2016; accepted: 29 December 2016)

Abstract: Despite its unique high efficiency and good environmental compatibility, the water-soluble binder system still encounters problems achieving a desired sintered part via ceramic injection molding because of the poor compatibility and the powder-binder segregation between ceramic powders and binders. The objective of this study was to obtain a sintered part with excellent properties by introducing a small quantity of oleic acid to the surface of zirconia powders before the mixing process. As opposed to many previous investigations that focused only on the rheological behavior and modification mechanism, the sintering behavior and densification process were systematically investigated in this study. With the modified powders, debound parts with a more homogeneous and smaller pore size distribution were fabricated. Also, a higher density and greater flexural strength were achieved in the sintered parts fabricated using the modified powders.

Keywords: ceramic materials; zirconia; injection molding; oleic acid; sintering

1. Introduction

Ceramic injection molding (CIM) is a fabrication technique that offers advantages for the mass production of intricate and precise ceramic parts at low cost; CIM has thus attracted extensive attention over the past several decades [1]. The CIM fabrication process starts with the blending process (i.e., blending of a mixture of organic vehicles and ceramic powders), followed by injection molding, binder (organic vehicles) elimination, and sintering [2]. The organic vehicles play a temporary but decisive role during the process, and determine the success or failure of a CIM production.

Binders utilized in CIM are typically composed of a major binder, a minor binder, a plasticizer/lubricant, and a small quantity of surfactant [3]. Because the particle size of the starting ceramic powders is usually in nanoscale range, the particles are prone to agglomeration, which introduces a challenge with respect to fabricating the desired parts by CIM. Thus, a small amount of surfactant is often added to the ceramic/binder mixtures to improve powder dispersion during the blending process, which ultimately leads to a higher solid loading and higher green strength without sacrificing the rheological behavior of the suspensions [4–5]. Recently, the most widely-used surfactants are coupling agents (e.g., silanes and titanates) and fatty acids (e.g., stearic acid (SA), oleic acid (OA), and 12-hydroxystearic acid (HSA)). With the introduction of these surfactants, feedstock with excellent homogeneity and less particle segregation was achieved due to the improved dispersion, compatibility, and rheological behavior of the suspensions [6].

Among the aforementioned surfactants, OA, because of its beneficial dispersion effect and low cost, has been widely investigated. For instance, Liu *et al.* [7] found that OA could form aluminum-oleate coating on the surface of γ-alumina powder and that the surface-modified γ-alumina suspension exhibited a better dispersion effect in octane compared to the effect of SA. Also, Liu [8] reported that OA strongly reduced the viscosity of zirconia–wax suspensions. Thistlethwaite *et al.* [9] investigated the interaction between OA and zirconia and reported that OA could preferentially adsorb onto the zirconia powder surface via a Lewis-type acid-base reaction or via an ion-exchange mechanism. Fur-

Corresponding author: Zhi-peng Xie E-mail: xzp@mail.tsinghua.edu.cn

thermore, Jeng *et al.* [10] introduced OA to CuO nanoparticles via a surface modified with OA to form cupric oleate and finally achieved fine dispersed CuO nanoparticles.

However, relevant researches on OA were limited to improving the dispersion of particles, reducing the viscosity of suspensions, and exploring the modification mechanism; by contrast, the effect of the incorporated OA on the final stage of the sintering process was rarely studied. In addition, previous studies on OA have primarily involved the wax-based binder system. The wax-based binder system usually introduces environmental challenges by its self-limitativeness. The organic binders can only be eliminated by thermal debinding (time-consuming) [11] or organic solvent debinding (the adopted organic solvents are generally toxic/carcinogenic) [12]. Consequently, the polyethylene glycol (PEG)-based binder system, as a non-toxic and commercially available water-soluble binder system, was adopted in this study. In the case of the PEG-based binder system, PEG can be first extracted by water to form the interconnected pore pathways through the part, which facilitate expulsion of the residual binders in the next thermal pyrolysis stage [13].

In this paper, different amounts (0.5wt%, 1.0wt%, 2.0wt%, and 3.0wt%) of OA were introduced to the zirconia powders prior to the blending process through a wet ball-milling treatment. The optimal addition of OA was confirmed by measurements of the contact angle between the modified dry-pressed body and the water/ethanediol polar solvents. The mechanism of modification was systematically discussed by Fourier Transform infrared spectroscopy (FTIR). With the modified powders, the debound part (after thermal debinding) exhibited a more homogeneous microstructure and a narrow pore size distribution. Also, greater density and higher flexural strength were achieved in the sintered part using modified powders. It was believed that the results of this investigation will improve the quality of CIM products using a water-soluble binder system.

2. Experimental

Zirconia powders of commercial purity, grade MS-FS-3.0 with an average particle size of 60 nm and a specific surface area of 14.38 m^2/g according to the supplier (Fanmeiya Advanced Materials Co., Ltd., Jiujiang, China), were used in this study. Their microstructure was presented in Fig. 1.

In this study, OA was introduced onto the zirconia powders before the blending process. The modification procedure was initiated by dissolving OA in ethyl alcohol with a mass ratio of 1:8 in a magnetic stirrer at an appropriate temperature (50°C). After the OA/alcohol mixture became clear and light yellow, the mixture was transferred to a polyurethane jar. The zirconia powders, which were first dried in an oven at 110°C for 6 h, were then gradually added to the OA/alcohol mixture (the additions of OA were 0.5wt%, 1.0wt%, 2.0wt%, and 3.0wt%) and the suspensions were conducted wet ball milling in a planetary ball mill for 16 h. To ensure that OA was coated onto the surface of zirconia powders, the suspensions were transferred to an oven for drying for 12 h at 130°C [14]. After pulverizing and sieving, the modified powders were then achieved.

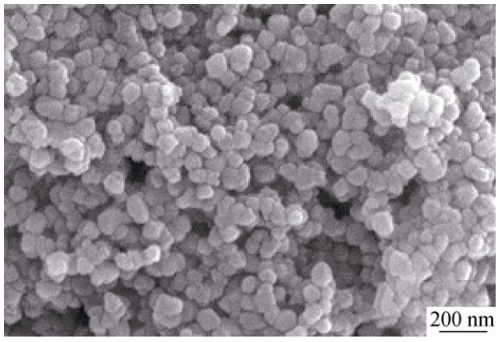

Fig. 1. Microstructure of zirconia powders observed by scanning electron microscopy.

The feedstock was prepared by blending the powders and binders in a twin screw kneader (SK-160, Shanghai Rubber Machinery, China) at 170–190°C for 30–40 min. The organic binders contained 61wt% polyethylene glycols (PEGS, consisted of 36wt% PEG 600 and 25wt% PEG 4000) as the major component, 25wt% polymethyl methacrylate (PMMA) as the backbone binder, 9wt% OA as the surfactant, 4.5wt% dibutyl phthalate (DBP) as the plasticizer, and 0.5wt% phenothiazine, as described by Yang *et al.* [15–16]. A small amount of phenothiazine was added to the suspension to prevent the oxidation of PEG in air [17]. The solid loading of the system was 50vol%; details of binder components are listed in Table 1.

Table 1. Contents and suppliers of the organic binder components utilized in this work

Component	Content / wt%	Supplier
PEG 600	36.0	Sinopharm Chemical Reagent Beijing Co. Ltd.
PEG4000	25.0	Sinopharm Chemical Reagent Beijing Co. Ltd.
PMMA	25.0	Degussa Co. Ltd.
OA	9.0	Sinopharm Chemical Reagent Co. Ltd.
DBP	4.5	Beijing Modern Eastern Fine Chemical Co. Ltd.
Phenothiazine	0.5	Shanghai Lindi Chemical Industry Co. Ltd.

Injection molding was carried out in an injection molding machine (JPH30/C/E, Qinchuan Hengyi Plastics Machinery Co. Ltd., China). Injected parts with dimensions of 5.0 mm × 6.0 mm × 50.0 mm were fabricated with the barrel temperatures between 160 and 180°C. A combination debinding process comprising water leaching to eliminate the PEG and thermal pyrolysis to remove residual binders was adopted in this study. During the water leaching, the green part was first immersed in distilled water at 45°C to eliminate approximately 80wt%–90wt% of the PEG. Then, the part was transferred to an oven and dried at 50°C. After the water leaching process, the interconnecting pores through the part were formed, which facilitated the next stage of thermal pyrolysis. The temperature and dwelling time of thermal pyrolysis were generally 600°C and 2 h, respectively. In order to study the sintering process, the debound bodies (after the debinding process) were then sintered at different temperatures (1000–1550°C at intervals of 50°C) for 2 h in air atmosphere.

The rheological properties of both feedstock with modified and unmodified powders were measured by a Bohlin, RH-7 Advanced Capillary Rheometer with a die of 1 mm in diameter (D), 16 mm in length (L) (L/D = 16). The test temperature, viscosity, and shear rates were 180°C, 10–500 Pa·s and 50–5000 s^{-1}, respectively. The wettability of water/ethanediol on the zirconia powders coated with different OA concentrations was determined by static contact-angle measurement (FTA 200, First Ten Angstroms, USA). For the measurements, the dry-pressed body plates utilizing the powders with various additions of OA (from 0.5wt% to 3.0wt%) were first prepared by a pressing machine. Then, a water/ethanediol drop was dripped onto the dry-pressed body plate with various amounts of OA (from 0.5wt% to 3.0wt%) to measure the contact angle by a contact-angle goniometer. Fourier transform infrared spectroscopy (FTIR-6700, Nicolet, USA) was used to characterize the powders. The morphological observations of the debound and sintered bodies were carried out by using field emission scanning electron microscopy (FESEM, MERUN VP COMPACT, Zeiss, Germany). The pore size distribution (PSD) of the debound bodies was evaluated by the mercury intrusion method (Autopore 9500, USA). The bulk densities of the sintered specimens were measured by the Archimedes method. To determine the flexural strength of the sintered parts at various temperatures, 3-point bending test was measured in a universal mechanical tester (AG-IC, Shimadzu, Japan). The dimensions of test bars were 3.0 mm × 4.0 mm × 36.0 mm.

3. Results and discussion

3.1. Determination of the optimal addition of OA

Fig. 2 shows the contact angle of water and ethanediol droplets on the dry-pressed body plates with different contents of OA. The contact angle depended critically on the addition of OA. The contact angle dramatically increased when the addition of OA was in the range of 0–2wt%, due mainly to the decrease in the surface tension of water/ethanediol upon the addition of OA. When the addition of OA was more than 2wt%, the contact angle trended to be steady. This can be attributed that the "actual" adsorption on the surface of the ceramic particle appeared to be saturated as the addition of OA was 2wt%. With the introduction of OA onto the ceramic particles, the polarity of the particles' surface could be changed from hydrophily to hydrophobicity, which was reflected by the decreases of the polar component and the dispersion component of the solid's surface tension, as shown in Table 2. The dependence of the contact angle on the polar and dispersion components is expressed using the following equation [18–19]:

$$\cos\theta = (2/\gamma_L)\left[(\gamma_{Lp}\gamma_{Sp})^{1/2} + (\gamma_{Ld}\gamma_{Sd})^{1/2}\right] - 1 \quad (1)$$

$$\gamma_S = \gamma_{Sp} + \gamma_{Sd} \quad (2)$$

where γ_L is the surface tension of the liquid, γ_{Lp} is the polar component of liquid's surface tension, γ_{Ld} is the dispersion component of the liquid's surface tension, γ_S is the surface tension of solid, γ_{Sp} is the polar component of the solid's surface tension, and γ_{Sd} is the dispersion component of the solid's surface tension.

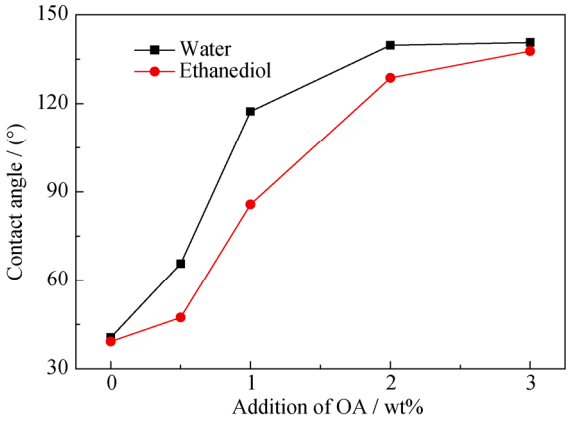

Fig. 2. Contact angle of water and ethanediol droplets on the dry-pressed body plates with various additions of OA.

Table 2. Surface tension of zirconia powders versus different additions of OA

Addition of OA / wt%	Contact angle (water) / (°)	Contact angle (ethanediol) / (°)	γ_{Sp} / (10^{-3} N·m^{-1})	γ_{Sd} / (10^{-3} N·m^{-1})	γ_S / (10^{-3} N·m^{-1})
0.0	40.50	39.17	2.92	57.72	60.64
0.5	65.63	47.29	1.88	20.21	22.09
1.0	117.29	85.67	0.28	1.01	1.29
2.0	139.09	128.68	0.06	0.06	0.12
3.0	140.63	137.72	0.05	0.61	0.66

Note: water ($\gamma_{Lp} = 51.0 \times 10^{-3}$ N·m^{-1}, $\gamma_{Ld} = 21.8 \times 10^{-3}$ N·m^{-1}); ethanediol ($\gamma_{Lp} = 19.0 \times 10^{-3}$ N·m^{-1}, $\gamma_{Ld} = 29.3 \times 10^{-3}$ N·m^{-1}).

3.2. Surface modification mechanism of OA onto zirconia powders

The above observations are attributed to the fact that OA had been absorbed on the surface of the zirconia particles, and this could also be supported by the FTIR results in Fig. 3, which offered the infrared absorption spectra of pure zirconia (ZrO_2) (Fig. 3(a)), modified ZrO_2 powder (Fig. 3(b)), and pure OA (Fig. 3(c)). In Fig. 3(a), the bands at 3438 and 507 cm^{-1} correspond to the vibration peak of hydroxyl (–OH) and show a strong amplitude, indicating that the surface of ZrO_2 was rich in hydroxyl groups and provided the possibility of ion-exchange or esterification with OA. Fig. 3(c) shows the infrared absorption spectrum of OA, in which the peak at 2850 and 2930 cm^{-1} correspond to long alkyl chains (–CH, –CH_2, and –CH_3). There is also a peak located at 1710 cm^{-1} corresponding to the carboxylate group (–COOH) [10]. Fig. 3(b) shows the infrared absorption spectrum of the ZrO_2 powder modified with 2wt% OA. The intensities of the hydroxyl vibration peaks (3438 and 507 cm^{-1}) are much weaker than those in the spectrum of pure ZrO_2, which implies that there is a chemical reaction between hydroxyl and carboxyl. The peak centered at 1385 cm^{-1} is attributed to the stretching vibration of C–O–C. Compared to the spectrum of pure zirconia (Fig. 3(a)), new absorption peaks appear at 1430 and 1548 cm^{-1} as shown in Fig. 3(b), which originate from 1710 cm^{-1} of OA, suggesting that a new compound (i.e., a carbonyl linked group –Zr–O–C–O) was formed on the surface of zirconia powders through the chemical reaction between OA and the ZrO_2 powder. Lee and Harris [20] and Liu *et al.* [21] considered that this reaction was an esterification process or ion-exchange reaction, expressed as:

$$ZrO_2(OH)_x + y(CH_3(CH_2)_7CH{=}CH(CH_2)_7COO)^- \longrightarrow ZrO_2(OH)_{x-y}((CH_2)_7CH{=}CH(CH_2)_7CH_3COO)_y + yOH^- \quad (3)$$

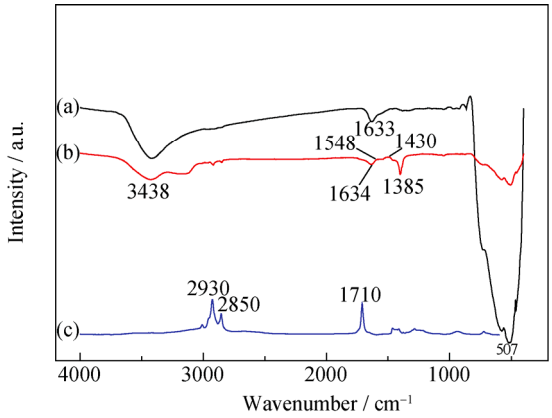

Fig. 3. Infrared spectra of (a) pure zirconia (ZrO_2), (b) modified ZrO_2 (2wt% OA), and (c) pure OA.

3.3. Effect of OA modification on the rheological behavior and PSD

Fig. 4 illustrates the rheological behavior of the unmodified powder and the modified powder at 180°C. Both samples showed shear thinning behavior (the viscosity decreased with increasing shear rate). Interestingly, at a given solid loading (50vol%), the suspension with the modified powder exhibited a lower viscosity than the unmodified one. On the basis of our previous work [6], we attributed this result to the better dispersion of the OA modified powders. Also, SEM micrographs and PSD of the debound part with various powders are presented in Fig. 5. A more homogeneous and intensive PSD microstructure was obtained in the debound part using modified powders, indicating that OA was effective to decrease the agglomeration of the powders. It was worth emphasizing that the debound part with a more intensive PSD would be beneficial to achieving a sintered part with higher density and fewer pores, as the densification would be much easier [22].

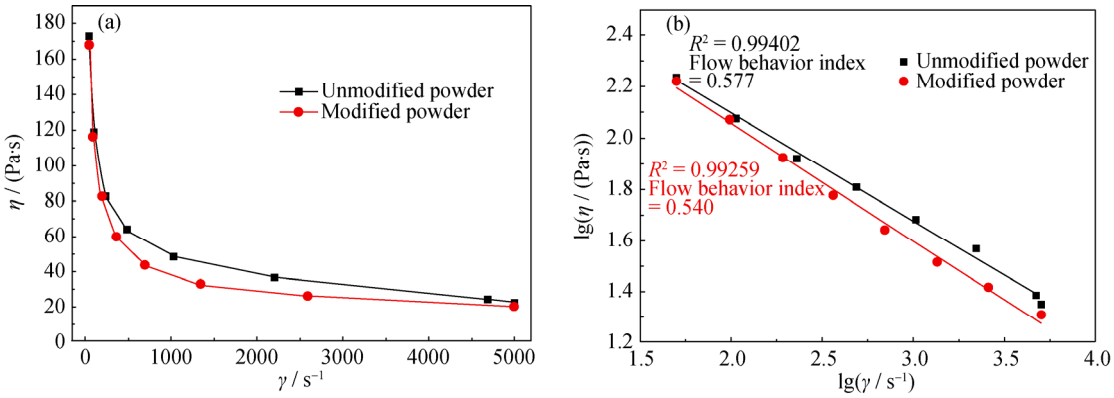

Fig. 4. Graphs of (a) viscosity (η) versus shear rate (γ) and (b) lgη versus lgγ for different powders at 180°C.

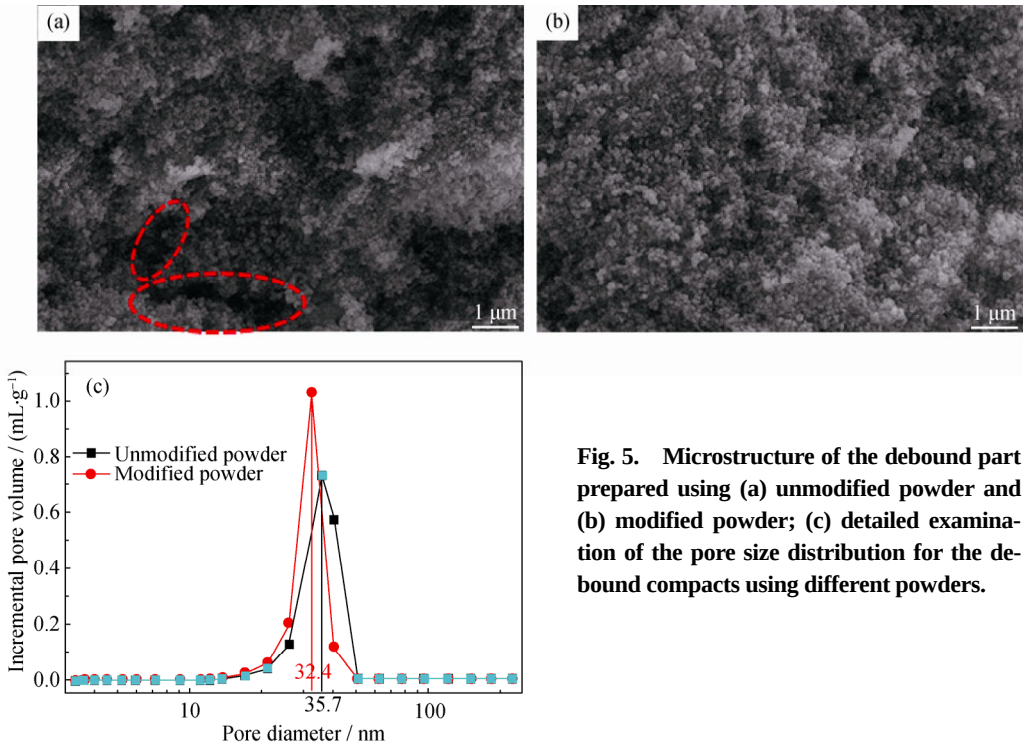

Fig. 5. Microstructure of the debound part prepared using (a) unmodified powder and (b) modified powder; (c) detailed examination of the pore size distribution for the debound compacts using different powders.

3.4. Effect of OA modification on the sintering behavior and densification process

Fig. 6 presents the relationship among the relative density, linear shrinkage, flexural strength, and sintering temperature for the unmodified and modified powders. For the two powders, the same densification process was observed, where the relative density increased with the increment of temperature in the range from 1000 to 1400°C and slightly declined with further increment of temperature above 1400°C. However, the part utilizing modified powders showed a higher density than the unmodified one at corresponding temperatures. In addition, in the range from 1000 to 1200°C, the part using modified powders exhibited greater shrinkage than the unmodified one. These results imply that within this temperature range, the densification of the modified powder was much more "thorough", thereby promoting "grains rearrangement" and pores removal, which is the prerequisite to achieving high density. However, when the sintering temperature was greater 1400°C, the density of both powders declined, and this could be attributed to an occurrence of oversintering. Also, the flexural strength of the zirconia ceramics exhibited the same trend, as shown in Fig. 6(b). Notably, the reduction extent of flexural strength for the modified ceramic was lower than that of the unmodified ceramic when the sintering temperature was greater than 1400°C, indicating that zirconia ceramics prepared using the modified powders exhibit more potential.

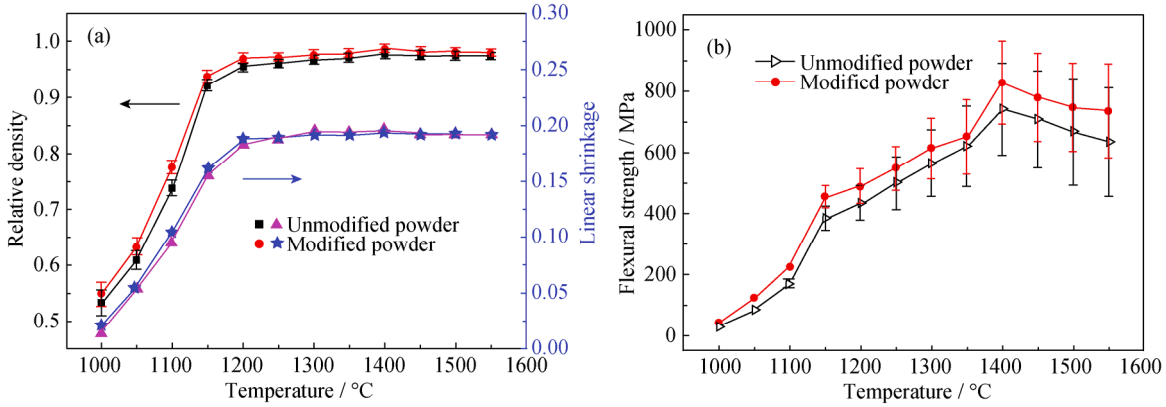

Fig. 6 Relationship among the relative density, linear shrinkage, and sintering temperature for unmodified and modified powders (a) and the flexural strength as a function of sintering temperature (b).

The sintering process can be divided into three stages on the basis of the specific microstructural features [23]: stage 1 (necks formation), stage 2 (porosity network formation), and stage 3 (closed porosity). With increasing the sintering temperature, the grain size and density also increased as shown in Fig. 7(c). Figs. 7(a) and 7(b) illustrate the microstructure of the two powders (unmodified powders and modified powders) in the different stages of the sintering process. During stage 1, the part using unmodified powders exhibited a more "unconfined" structure than the modified ones. In addition, large holes and particle segregation were easily observed in the unmodified part. As sintering proceeded, the density and grain size of both parts gradually grew. As the holes presented in stage 1 were too large to be "cured", voids appeared during stage 2 in the case of the part using unmodified powders. When the process reached stage 3, these voids had been "mitigated", however, the small pores were still present and thus prevented the sintered part from achieving excellent mechanical properties. For the part using modified powders, as the dispersion was improved by the modification of OA, the particle segregation in stage 1 was weaken. In the following stage 2, as the distance among zirconia particles became small, a more homogeneous structure was easily obtained. At an appropriate sintering temperature, a uniform microstructure with fine grain size was achieved in stage 3.

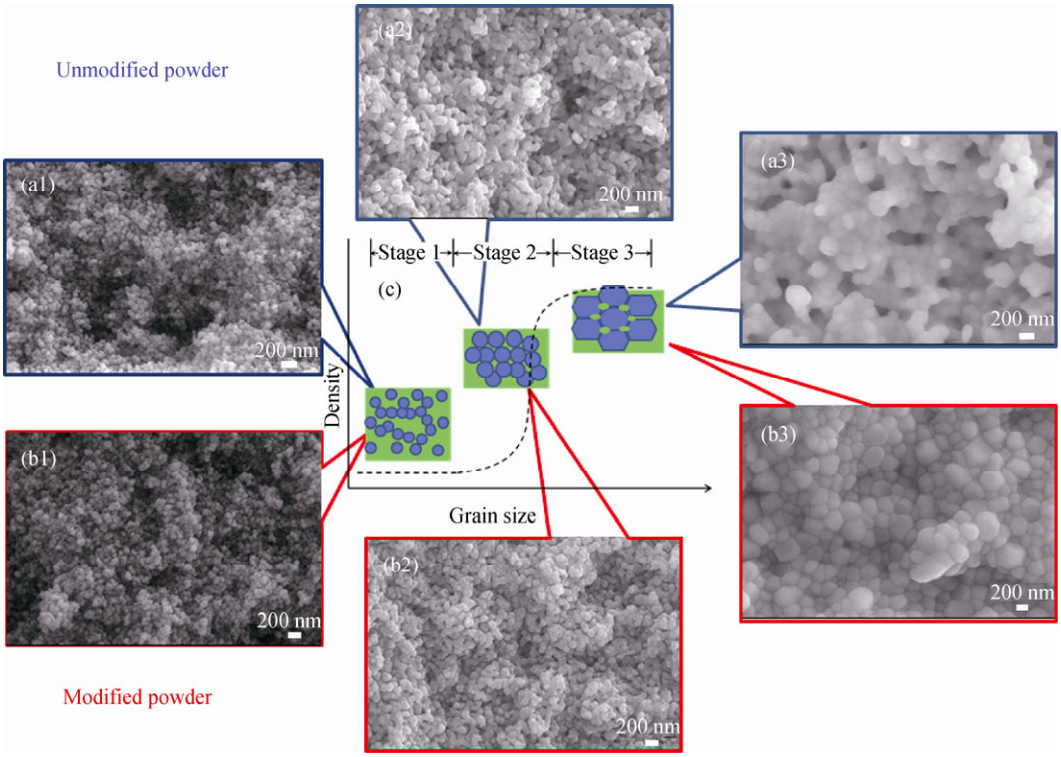

Fig. 7. Unmodified powders in the different periods of the sintering process: (a1) stage 1; (a2) stage 2; (a3) stage 3. Modified powders in the various periods of the densification process: (b1) stage 1; (b2) stage 2; (b3) stage 3. (c) Schematic of the sintering process.

To further affirm the proper sintering temperature of the part using modified powders, the microstructure of sintered bodies (from 1350 to 1550°C) which had been thermally etched and the relationship among the relative density, average grain size, and sintering temperature are presented in Fig. 8. According to Fig. 8(f), the density and grain size increased with increasing temperature. Especially, extensive grain growth was observed above 1400°C, as also evidenced in Figs. 8(a)–8(e). With the increase of temperature (from 1450 to 1550°C), abnormal growth of grains began to appear in some local region due to the exorbitant sintering driving force. More seriously, the excessive sintering temperature resulted in some grains growing too large, and the size actually reached 1 μm at 1550°C, which was detrimental to the mechanical properties of the zirconia ceramics (as shown in Fig. 6(b)). By comparing the microstructures of zirconia ceramics sintered at five sintering temperatures, no significant pores or abnormal grain growth was observed in the part sintered at 1400°C where the average grain size was ~230 nm. Also, the optimal mechanical properties were achieved at this temperature (as shown in Fig. 6(b)).

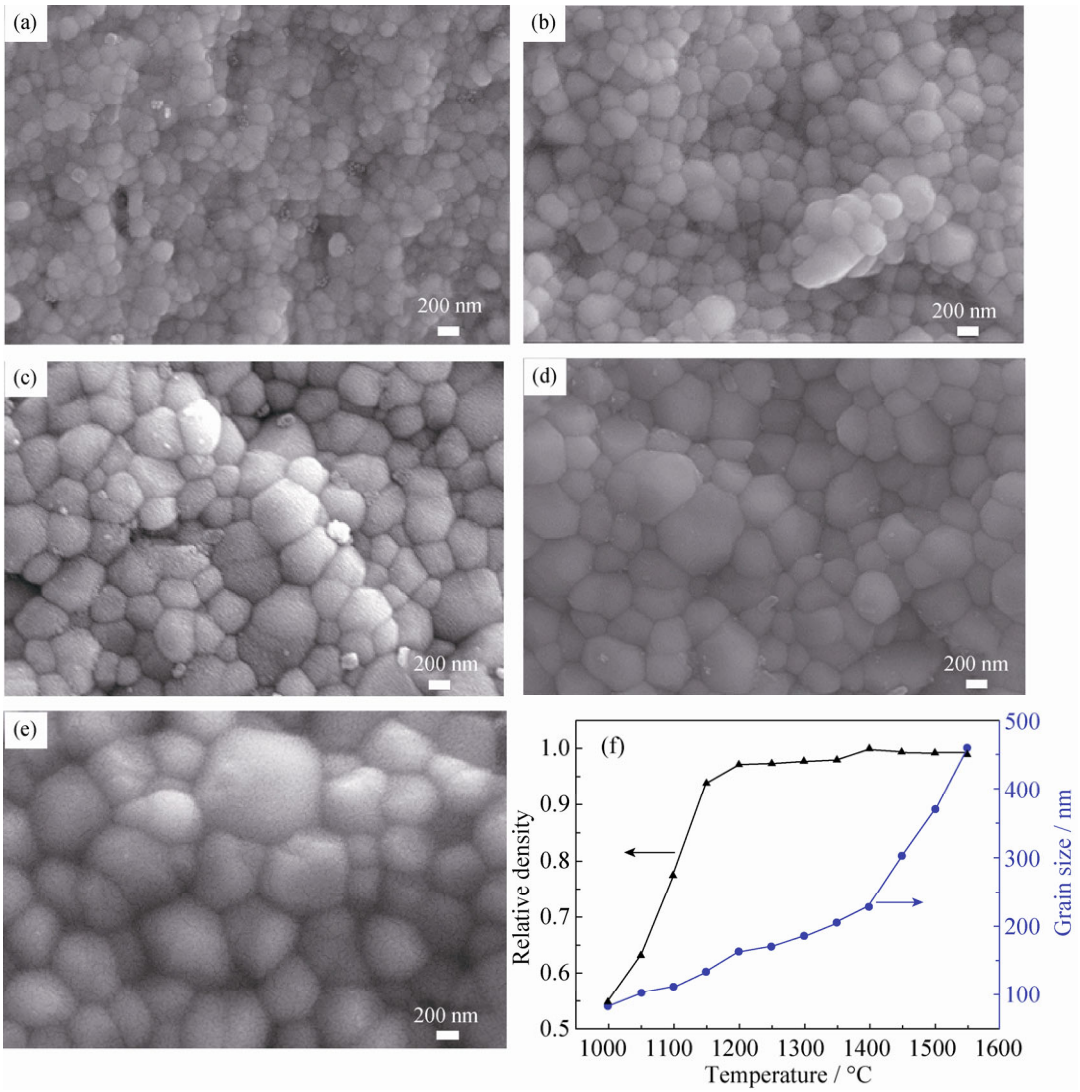

Fig. 8. Microstructure of the sintered zirconia ceramics using modified zirconia powders at various sintering temperatures: (a) 1350°C; (b) 1400°C; (c) 1450°C; (d) 1500°C; (e) 1550°C. (f) Relationship among the relative density, average grain size, and sintering temperature.

4. Conclusion

A systematic investigation of the surface modification strategy of OA in the PEG-based binder system for CIM was carried out. The results of contact angle measurements indicated that the optimum amount of the OA addition was 2wt%. The polarity of the ceramic surface was changed from hydrophilic to hydrophobic after the surface modifica-

tion with OA. FTIR analysis indicated that the OA interacted with the zirconia powder by an esterification process or ion-exchange mechanism. After the whole debinding process, the debound part using modified powders exhibited a more homogeneous microstructure and narrower PSD than unmodified ones. A greater relative density and higher flexural strength were achieved in the sintered body using the modified powders, and the highest values were obtained at 1400°C. Also, a homogenous microstructure with an average size of 230 nm and no abnormal grain growth were achieved at this temperature. In summary, OA not only improved the rheological behavior and homogeneity of the suspension but also promoted densification and enhanced the mechanical properties of the sintered zirconia ceramics using the PEG-based binder system.

Acknowledgements

This work was financially supported by the National Natural Science Foundation of China (Nos. 51572035 and 51502041).

References

[1] V. Piotter, M. Beck, K. Plewa, H.J. Ritzhaupt-Kleissl, A. Ruh, and J. Hausselt, Micro PIM moves into the zone of industrial possibility, *Met. Powder Rep.*, 64 (2009), No. 9, p. 35.

[2] B.C. Mutsuddy, Injection molding, [in] *Engineered Materials Handbook Volume 4*: *Ceramics and Glasses*, Edited by D.W. Richerson, ASM International, Ann Arbor, 1991, p. 173.

[3] D.M. Liu and W.J. Tseng, Yield behavior of zirconia-wax suspensions, *Mater. Sci. Eng. A*, 254(1998), No. 1-2, p. 136.

[4] W. Liu, Z.P. Xie, T.Z. Bo, and X.F. Yang, Injection molding of surface modified powders with high solid loading: a case for fabrication of translucent alumina ceramics, *J. Eur. Ceram. Soc.*, 31(2011), No. 9, p. 1611.

[5] X.F. Yang, J.H. Yang, X.W. Xu, Q.C. Liu, Z.P. Xie, and W. Liu, Injection molding of ultra-fine Si_3N_4 powder for gas-pressure sintering, *Int. J. Miner. Metall. Mater.*, 22(2015), No. 6, p. 654.

[6] J.X. Wen, Z.P. Xie, and W.B. Cao, Novel fabrication of more homogeneous water-soluble binder system feedstock by surface modification of oleic acid, *Ceram. Int.*, 42(2016), No. 14, p. 15530.

[7] J.C. Liu, J.H. Jean, and C.C. Li, Dispersion of nano-sized γ-alumina powder in non-polar solvents, *J. Am. Ceram. Soc.*, 89(2006), No. 3, p. 882.

[8] D.M. Liu, Effect of dispersants on the rheological behavior of zirconia-wax suspensions, *J. Am. Ceram. Soc.*, 82(1999), No. 5, p. 1162.

[9] P.J. Thistlethwaite, M.L. Gee, and D. Wilson, Diffuse reflectance infrared Fourier transform spectroscopic studies of the adsorption of oleate/oleic acid onto zirconia, *Langmuir*, 12(1996), No. 26, p. 6487.

[10] J.Y. Jeng, J.C. Liu, and J.H. Jean, Dispersion of oleate-modified CuO nanoparticles in a nonpolar solvent, *J. Am. Ceram. Soc.*, 90(2007), No. 11, p. 3676.

[11] W.W. Yang and M.H. Hon, *In situ* evaluation of dimensional variations during water extraction from alumina injection-molded parts, *J. Eur. Ceram. Soc.*, 20(2000), No. 7, p. 851.

[12] C.F. Escobar and L.A. dos Santos, New eco-friendly binder based on natural rubber for ceramic injection molding process, *J. Eur. Ceram. Soc.*, 35(2015), No. 13, p. 3567.

[13] V.A. Krauss, A.A.M. Oliveira, A.N. Klein, H.A. Al-Qureshi, and M.C. Fredel, A model for PEG removal from alumina injection molded parts by solvent debinding, *J. Mater. Process. Technol.*, 182(2006), No. 1-3, p. 268.

[14] W.J. Tseng, D.M. Liu, and C.K. Hsu, Influence of stearic acid on suspension structure and green microstructure of injection-molded zirconia ceramics, *Ceram. Int*., 25(1999), No. 2, p. 191.

[15] X.F. Yang, W. Liu, Z.P. Xie, and X.W. Xu, Optimization of the compositions of PEG/PMMA binder system in ceramic injection moulding via water-debinding, *Appl. Mech. Mater.*, 302(2013), p. 556.

[16] X.F. Yang, C. Jia, Z.P. Xie, W. Liu, and Q.C. Liu, Water-soluble binder system based on poly-methyl methacrylate and poly-ethylene glycol for injection molding of large-sized ceramic parts, *Int. J. Appl. Ceram. Technol.*, 10(2013), No. 2, p. 339.

[17] W. Liu, Z.P. Xie, and C. Jia, Surface modification of ceramic powders by titanate coupling agent for injection molding using partially water soluble binder system, *J. Eur. Ceram. Soc.*, 32 (2012), No. 5, p. 1001.

[18] S.H. Wu, Calculation of interfacial tension in polymer systems, *J. Polym. Sci. Polym. Symp.*, 34 (1971), No. 1, p. 19.

[19] S.H. Wu, Surface and interfacial tensions of polymer melts: II. Poly(methyl methacrylate), poly(*n*-butyl methacrylate), and polystyrene, *J. Phys. Chem.*, 74(1970), p. 632.

[20] S.Y. Lee and M.T. Harris, Surface modification of magnetic nanoparticles capped by oleic acids: characterization and colloidal stability in polar solvents, *J. Colloid Interface Sci.*, 293(2006), No. 2, p. 401.

[21] W. Liu, Z.P. Xie, X.F. Yang, Y. Wu, C. Jia, T.Z. Bo, and L.L. Wang. Surface modification mechanism of stearic acid to zirconia powders induced by ball milling for water-based injection molding, *J. Am. Ceram. Soc.*, 94(2011), No. 5, p. 1327.

[22] C.J. Tsai, C.N. Chen, and W.J. Tseng, Rheology, structure, and sintering of zirconia suspensions with pyrogallol-poly(ethylene glycol) as polymeric surfactant, *J. Eur. Ceram. Soc.*, 33(2013), No. 15-16, p. 3177.

[23] M.J. Mayo, Processing of nanocrystalline ceramics from ultrafine particles, *Int. Mater. Rev.*, 41(1996), No. 3, p. 85.